Submitted to the 1993 Particle Accelerator Conference
Washington, D. C., May 17-20 1993

BNL-48678

Low Energy Beam Transport in the NSLS UV-FEL *

Xiaohao Zhang and Juan C. Gallardo
National Synchrotron Light Source and Physics Department
Brookhaven National Laboratory
Upton, NY 11973

Abstract

We present a design of the injection low energy transport line for the proposed NSLS UV-FEL. The main concern is to control the beam transverse emittance dilution due to space charge, energy spread and non-linear forces introduced by magnetic elements. In this paper, we discuss the design considerations to optimize the transport line including the deleterious effects of space charge and energy spread as modeled by the particle code PARMELA. The results from PARMELA are analyzed and the concept of slice emittance is used to examine the causes of emittance growth.

I Introduction

The National Synchrotron Light Source (NSLS) at BNL is proposing the construction of a UV free electron laser (UV-FEL) radiation source capable of providing tunable, coherent radiation from 3000 Å to 750 Å at near gigawatt peak power. [1] Such a source with peak energy near 1 mJ per pulse is well beyond conventional laser technology and could have an immediate impact on a large number of experimental studies in a varied of fields in physics, chemistry and biology. [2]

The proposed FEL is a subharmonically seeded single pass FEL using harmonic generation techniques, which utilizes two wiggler magnets separated by a dispersion section. [3] This technique can provide short wavelength, high peak power and very stable radiation.

The FEL is expected to be driven by a 300 Å conventional seed laser and a 260 MeV energy electron beam with 8π mm-mrad normalized rms emittance and a local

*This work was performed under the auspices of the U.S. Department of Energy, under Contract No. DE-AC02-76CH00016.

0.1% energy spread. The accelerator used to achieve such a beam is a superconducting recirculating linac system. An schematic of the machine shown in Fig. 1 consists of a 10 $\sim$ 20 MeV injector, a superconducting linac segment, a recirculator, and a separating/matching section.[4] The electron beam is recirculated to make up to three passes through the linac segment. The linac accelerates the beam with an energy gain of 80 MeV per pass to a final energy of 260 MeV. There are two recirculation lines (100 MeV and 180 MeV) to transport the beam back to the linac for further acceleration. Each recirculation line consists of two arcs and a transformer. The final part of the transport line is used to switch the beam to different wigglers and to match the beam at the entrance of each wiggler to the required FEL parameter.

In this paper we are focussing on the low energy beam injection line which starts from the exit of a photocathode electron gun to the entrance of the superconducting linac segment. The design considerations concerning emittance are discussed in section II. A detailed optics design of the line based on the code PARMELA [5] in conjunction with code TRACE3D [6] is presented in section III. In section IV, the result from PARMELA are discussed and analyzed making use of the concept of slice emittance.

II Design Consideration

The physics of free electron laser requires the electron beam emittance $\epsilon_n < \lambda$. The emittance growth in the entire transport line is mainly taking place in the low energy transport line. Therefore, a major concern in the design of the low energy injection line is to minimize the electron beam emittance growth. The emittance discussed here is the rms normalized emittance defined by

$$\epsilon_n = \sqrt{< x^2 >< p_x^2 > - < xp_x >^2} \quad [\pi\,\mathrm{mm} - \mathrm{mrad}]$$

in the projected two-dimensional phase space. In a linear system, in which horizontal (x), vertical (y) and longitudinal (z) motion are decoupled, the emittance is a invariant in absence of energy spread. The emittance dilution is the result of nonlinearity of magnetic elements, energy spread, space charge, and the coupling between x, y and z phase spaces. In addition the emittance growth can also be caused by a mismatched beam.

The magnetic nonlinearity can be caused either by nonlinear devices or by the edge or end effects of linear devices without considering the distortion or error of the magnets themselves. The coupling of the phase space planes is intrinsic to the dynamics of the RF electron gun and to the external magnetic focussing forces. To minimize the emittance dilution due to nonlinear magnetic field, the transport line is designed with only linear elements with no coupling and the size of the beam is kept small in the good field regions.

The canonical definition of the emittance makes it non-constant even in drift spaces when the beam has energy spread; this fact is not present in the unnormalized

definition . The emittance variation arising from energy spread depends on the the transverse velocities of the beam. To minimize the emittance dilution, it is best to maintain the beam parallel to the propagation axis, over focussing should be avoided.

A major cause of emittance growth in low energy beam is the space charge force. This Coulomb self force is complicated because the field depends upon the time(phase)-varying charge density of the beam; in general, it is nonlinear and time dependent. It also enhances energy spread and generates coupling between the three phase space planes. In turn these nonlinearity, energy spread and coupling produce an emittance increase. The emittance increment due to the space charge is proportional to beam size and inversely proportional to the third power of the beam energy. To minimize the space charge effects for emittance preservation, it is desirable to go to high energy immediatelyafter the gun and to keep the beam size small.

III Transport Line Description

The low energy beam transport line from the end of the photocathode rf gun to the entrance of the superconducting linac is shown in Fig. 2. This 10 meter long line can be separated into two distinct parts, an accelerator section and a 45° bend section. Each section is about 5 meter long.

The input beam is adopted from simulations of a 3-$\frac{1}{2}$ cell photocathode RF gun,[7] as generated by the particle-in-cell code MAGIC [8]. The parameters of the input beam are listed in Table 1[9]. The initial beam profiles in phase space are shown in Fig. 3 where the average slope $< rr' > / < r^2 >$ has been substracted to exhibit the fan-like structure of the beam. The output of MAGIC is used as an input to the three-dimensional code PARMELA with a two dimensional space charge model. PARMELA is the chosen design code for the low energy transport line in conjunction with the transfer matrix base code TRACE3D.

The accelerator section consist of a solenoid and a superconducting RF cavity. The solenoid is needed to provide equal focusing in both transverse directions and convert the divergent beam into a convergent beam. The superconducting cavity has two 4-cell accelerating parts separated by a one rf wavelength drift distance. This cavity is used to increase the beam energy from 10 MeV to 20 MeV in order to reduce space charge effects.

The length and strength of the solenoid is adjusted to present a convergent beam to the superconducting cavity and to focus the beam to a waist at the first dipole of the bend. This arrangement smooths the beam envelope and reduces the emittance growth; also, it provides a necessary matching for the beam entering the bend. In Fig. 4, we show the electron envelope for the accelerating section.

The initial beam pulse length is about 2 ps which is equivalent to 0.36° of RF phase at 500 MHz. Since the pulse length is just one-thousandth of the RF wavelength, the energy spread induced by the cavity is negligible. To have the maximum acceleration, the beam is placed on the peak of the RF field. This gives relatively

Table 1: Injected Beam Parameters

Energy, [MeV]	9.5
Charge, [nC]	1.0
Normalized RMS Emittance x,[mm-mrad]	3.23
Normalized RMS Emittance y,[mm-mrad]	2.92
Longitudinal RMS Emittance,[KeV-deg]	2.78
Horizontal Beam Radius [mm]	3.50
Vertical Beam Radius [mm]	3.55
Pulse Length [ps]	1.87
Horizontal Beam Div.[mrad]	8.16
Vertical Beam Div.[mrad]	8.30
RMS Energy Spread [%]	0.39

smaller transverse emittance but larger energy spread arising from longitudinal space charge forces. A different choice is to place the beam off peak field, accelerate the tail of the pulse with the field larger than that of the front to compensate the effects due to longitudinal space charge; however, this in turn gives larger transverse emittance.

The 45° bend section is necessary to reinject the beam into the superconducting linac. This bend consists of three 15° dipoles, which is needed for an isochronous condition. The last dipole is a common dipole used in both the injection bend and the reinjection chicane. A 0.8 meter long drift space is required before the last dipole to avoid physical interference between the two lines. There are quadrupole triplets in between the dipole magnets to provide proper focusing and to achieve achromatic and isochronous bending. The beam envelopes for the bend are shown in Fig. 5. Without space charge, the section is symmetric about the center of the middle dipole. The system is tuned to be achromatic and isochronous. The symmetry is broken when space charge is taken into account. In order to make first order transport elements R_{16}, R_{26} and R_{56} to be zero with space charge, the quadrupoles are decoupled and retuned. This study has been completed using the code TRACE3D and verified with PARMELA. With 500 mA beam current, which is equivalent to 1 nC in the bunch, the system is *almost* achromatic and isochronous. The envelope of the beam remains small and smooth. The emittance dilution due to mismatching caused by linear space charge is insignificant.

IV PARMELA Results

In this section, PARMELA results based on the optics described in previous section are discussed. We begin to examine the emittance dilutions due to different effects.

We then analyze the results introducing the concept of slice emittance.

In the Fig. 6 the beam envelopes from PARMELA in both horizontal and vertical direction are shown. These are in a good agreement with the results from TRACE3D (Note there is a factor of $\sqrt{5}$ difference between the radius given by PARMELA and that given by TRACE3D.). The pulse length and absolute energy difference are displayed in Fig. 7 and 8. The pulse length increases from 1.87 ps to 2.25 ps in this low energy beam line; the value of the global energy spread is 37 KeV at the start and 181 KeV at the end.

The causes of the emittance growth in low energy injection line were discussed in general in section II. Using the code PARMELA, we are able to examine the emittance dilution due to each of those effects. We start with a beam with no energy spread and zero space charge, the only source of emittance growth is coming from the nonlinearity of the magnetic elements and the couplings present at the end of the rf electron gun (1). We then add natural energy spread (2) back to the injected beam but not space charge to examine its effects on the emittance. Finally, the space charge self force is turned on and we investigate first the effects due to the space charge nonlinearity and coupling (3), then the effects due to the space charge induced energy spread (4). To examine these different effects on emittance growth we show the horizontal and vertical emittances vs longitudinal distance in Fig. 9 and 10 respectively.

As expected, the effects due to the initial coupling and the nonlinearity in the magnets on transverse emittance growth is weak, since there is no nonlinear element in the transport line. If the errors of magnetic elements are introduced, some nonlinearity will show up and this effect may become stronger. The emittance growth due to natural energy spread (about 0.4%) is responsible for the initial fast emittance growth. This effect depends on both the energy spread and the transverse divergence of the beam, which is about 8.3 mrad in both transverse plane for our case. To reduce this effect, the beam with small energy spread and small angle divergence is desirable.

When the space charge effect is included, the strengths of the solenoid and the quadrupoles are readjusted to achieve the beam waist at the first dipole magnet and isochronous condition. A similar behavior of the emittance in both horizontal and vertical planes before the bend is observed with or without the space charge induced energy spread. Therefore, the emittance dilution in this part is mainly due to the nonlinear forces and coupling introduced by the space charge. Inside the bend, the vertical emittance grows almost linearly with axial distance.

The difference between the case when we include space charge induced energy spread and the case of excluding it, is coming from the chromatic effects due to the space charge, since the focussing strength is energy dependent. The horizontal emittance is different from the vertical one because of dispersion.

When the beam passes through dipole magnets, the emittance was observed to jump. The value of the jump depends on the energy spread and phase space shape of the beam. In the case with space charge induced energy spread, the energy spread at the first dipole is 0.57% instead of 0.17% for the case without space charge induced

energy spread. And the energy spread increase to 0.71% at the middle dipole and to 0.83% at the last dipole. In this case the energy spread makes strong chromatic effects. Furthermore, the achromatic and isochonous conditions are difficult to achieve in this case. As a result, the emittance is hard to be totally recovered after the final bend. To minimum these effects, it is desirable that the beam has a waist at each dipole magnet. A shorter achromatic bend and small dispersion are preferred, which translate into an smaller bending angle and radius. Finally, over focussing should be avoided for the emittance increase due to energy spread and large angle divergence.

The emittance discussed so far is the overall emittance of the entire electron bunch. However, the more important quantity for an FEL is an axial slice emittance and the corresponding current. The concept of slice emittance of the beam has been emphasized in Ref.[10] and [11]. In the case we are studying each slice has a very small emittance, but the overall emittance of the beam is larger as different slices project ellipsis of different orientation in the transverse phase space (x,x'), yielding a significant larger total ellipse.

The main responsible for the slice emittance differences is the space charge which acts differently as we move along the length of the pulse. The back and the front of the electron pulse have in general larger ellipses than the core of the beam. In our studies we have divided the electron pulse into five slices of equal extend and computed the transverse and longitudinal emittance and the current carried by each of them.

The beam at the end of the injection line is shown in Fig. 11. In x-y plane, the beam is seen as a solid spot with a halo. If the beam pulse is divided longitudinally into five equal slices, the particles in the halo are mainly from the last slice. In the transverse phase space, these particles occupy a much larger area in phase space and consequently they makes a significant contribution to the total emittance. In Table 2, the emittance and current of each slice at end of the transport line are listed. If the last slice containing about 6% of the particles is discarded, The beam satisfy the FEL emittance requirements although the current is still below the specified value of 300 A. Present studies with 2 nC indicate that it will be possible to satisfy the FEL constraints on current and emittance.

Table 2: Slice emittances and current.

slice	ϵ_x (mm-mrad)	ϵ_y (mm-mrad)	ϵ_z (KeV-deg)	I_{slice} (A)
1	2.486	4.524	5.980	61.8
2	3.382	3.215	5.110	115.3
3	6.913	1.843	8.097	158.4
4	7.052	7.989	4.627	115.0
5	13.337	10.955	4.099	28.7

V Conclusions

We have presented the design of a low energy transport line for the proposed UV-FEL at BNL. We have used the output of the 3-D fully relativistic code MAGIC as an input for the simulation codes which include space charge, PARMELA and TRACE3D. Detailed simulations show that is possible to transport a 1-nC electron beam without serious emittance dilution if we ignore the contribution of the back of the pulse (less than 6% of the charge).

ACKNOWLEDGEMENTS

We would like to thank R. B. Palmer and I. Ben-Zvi for illuminating discussions, and G. D. Warren for providing MAGIC output files. The authors would also like to acknowledge the contribution of S. Kramer in the initial stage of this work.

References

[1] I. Ben-Zvi, et al., Nucl. Instr. & Meth. **A318**, 201(1992).

[2] I. Ben-Zvi, et al., Nucl. Instr. & Meth. **A304**, 181(1991).

[3] L. H. Yu, Physical Review A 44 5178(1991).

[4] X. Zhang, et al., Proc. of 3rd EPAC, 1530(1992).

[5] L. Young, Private communication.

[6] K. R. Crandall, Trace 3-D version on VAX/VMS, LA-UR-90-4146 Los Alamos Accelerator Code Group, second edition Dec. 1990.

[7] I. S. Lehrman, et al., Nucl. Instr. & Meth. A318, 247 (1992).

[8] G. D. Warren, et al., Proc. Conf. on Computer Codes and the Linear Accelerator Community, Los Alamos National Laboratory, Jan. 22-25, 1990, ed. R. Cooper, LA-11857-C.

[9] G. D. Warren, Private communication.

[10] J. C. Gallardo, et al., IEEE J. of Quantum Electron. **QE-26**, 1328(1990).

[11] R. L. Sheffield, et al., Nucl. Instr. & Meth. A318, 282 (1992).

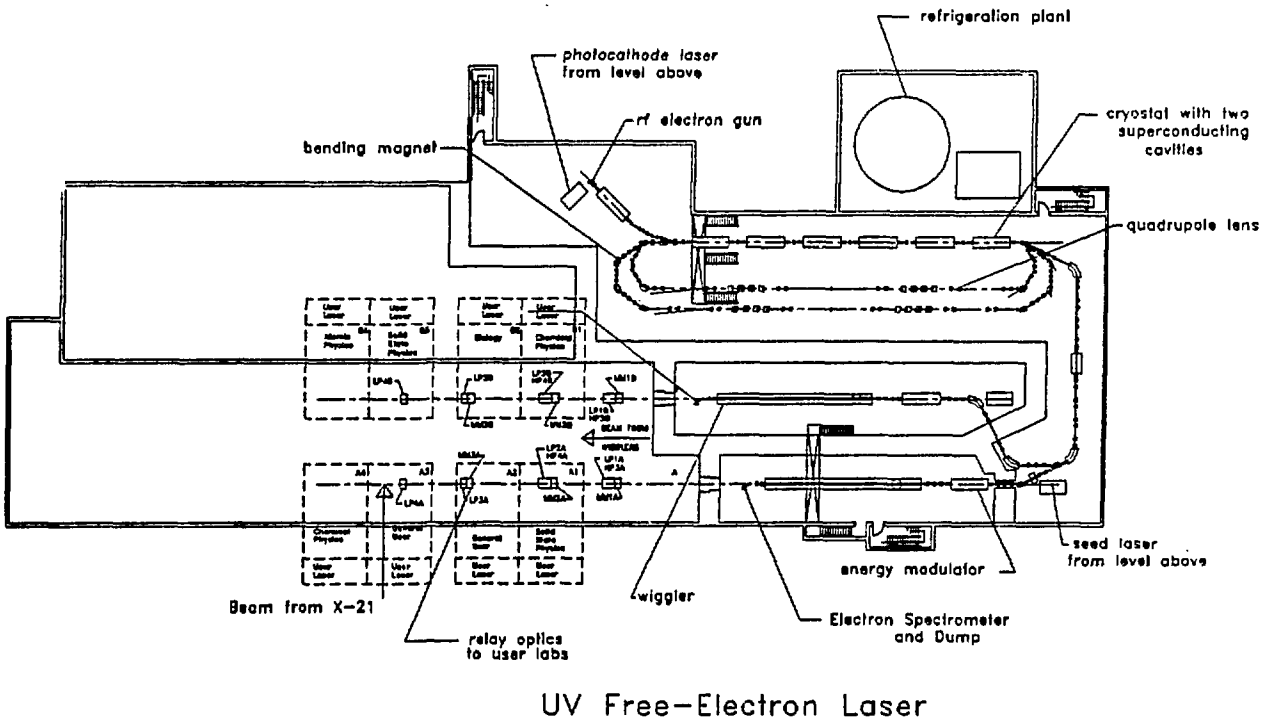

Figure 1: Schematic layout of NSLS UV-FEL.

DISCLAIMER

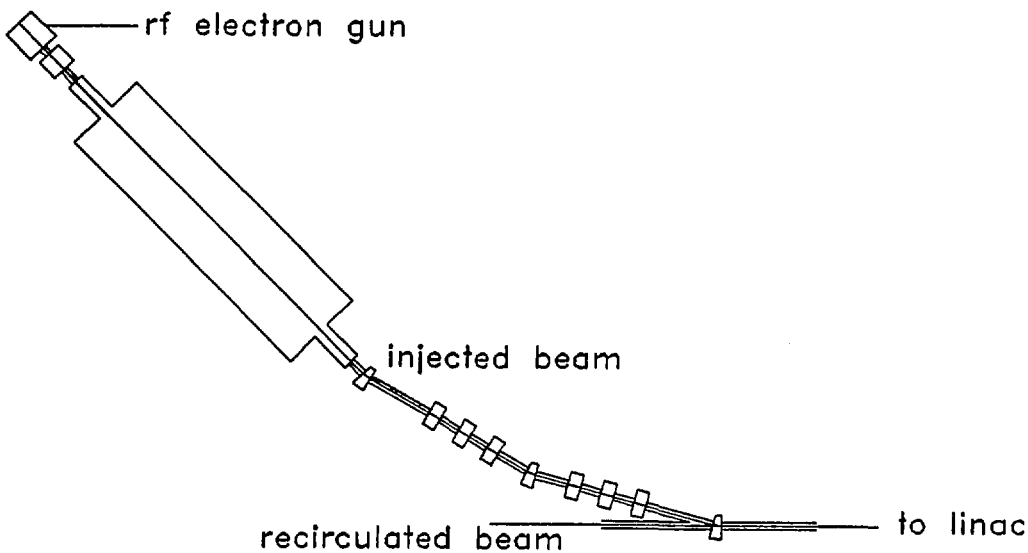

Figure 2: Schematic of the low energy beam transport line.

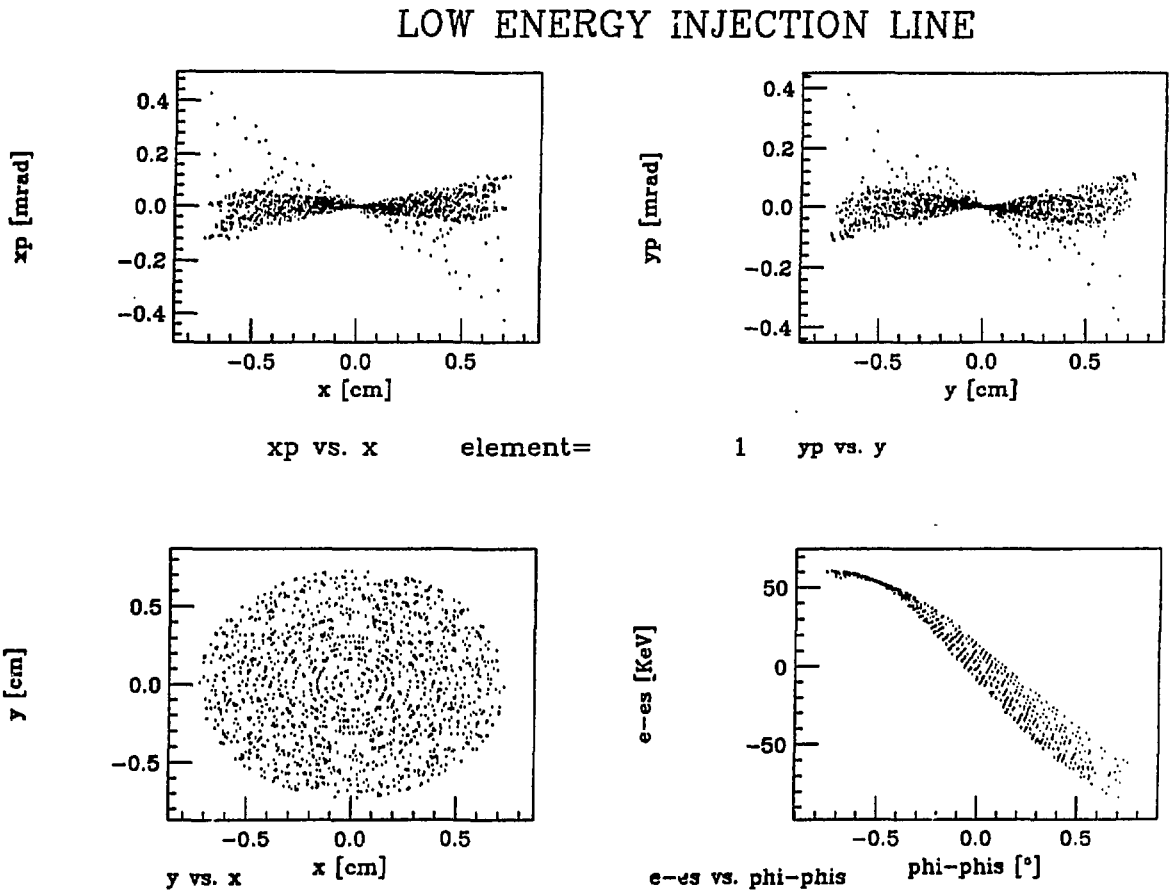

Figure 3: Phase space plots at the exit of the gun (MAGIC output).

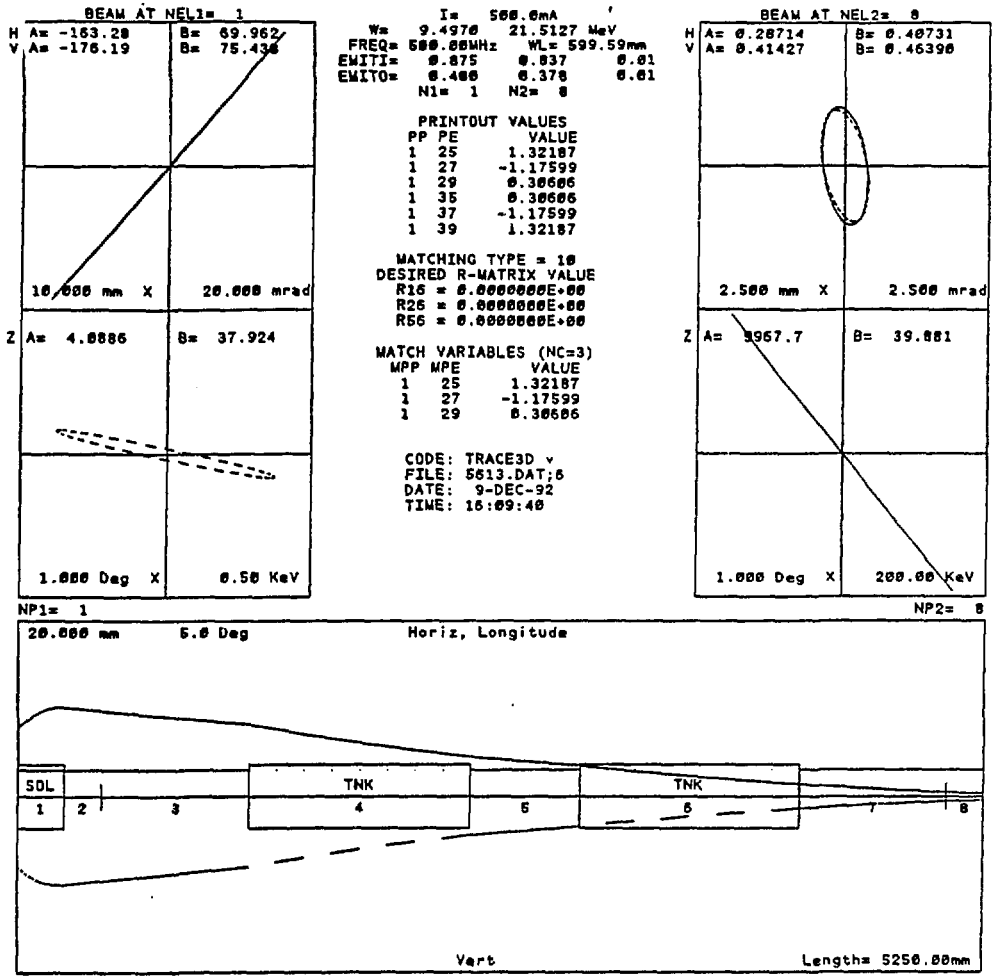

Figure 4: Beam envelope in the accelerating section.

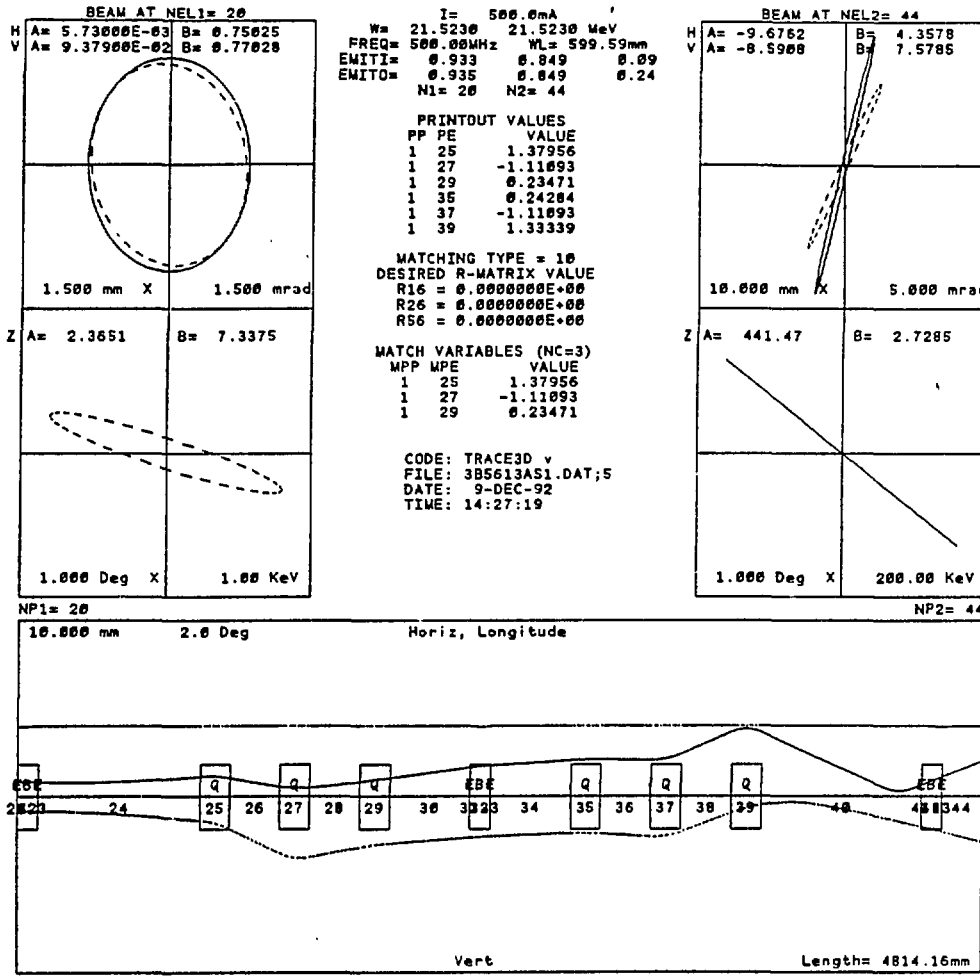

Figure 5: Beam envelope in the bend section.

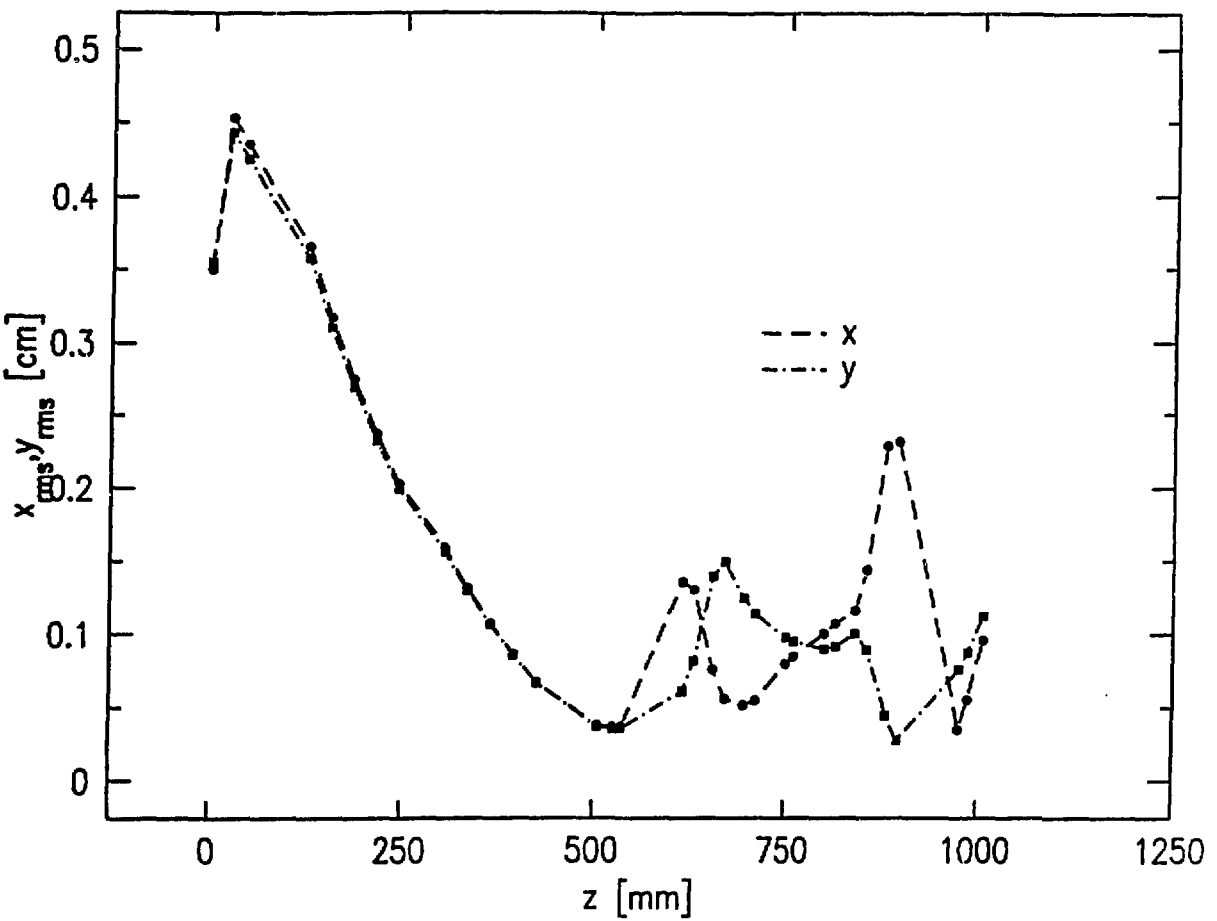

Figure 6: Beam envelope from PARMELA.

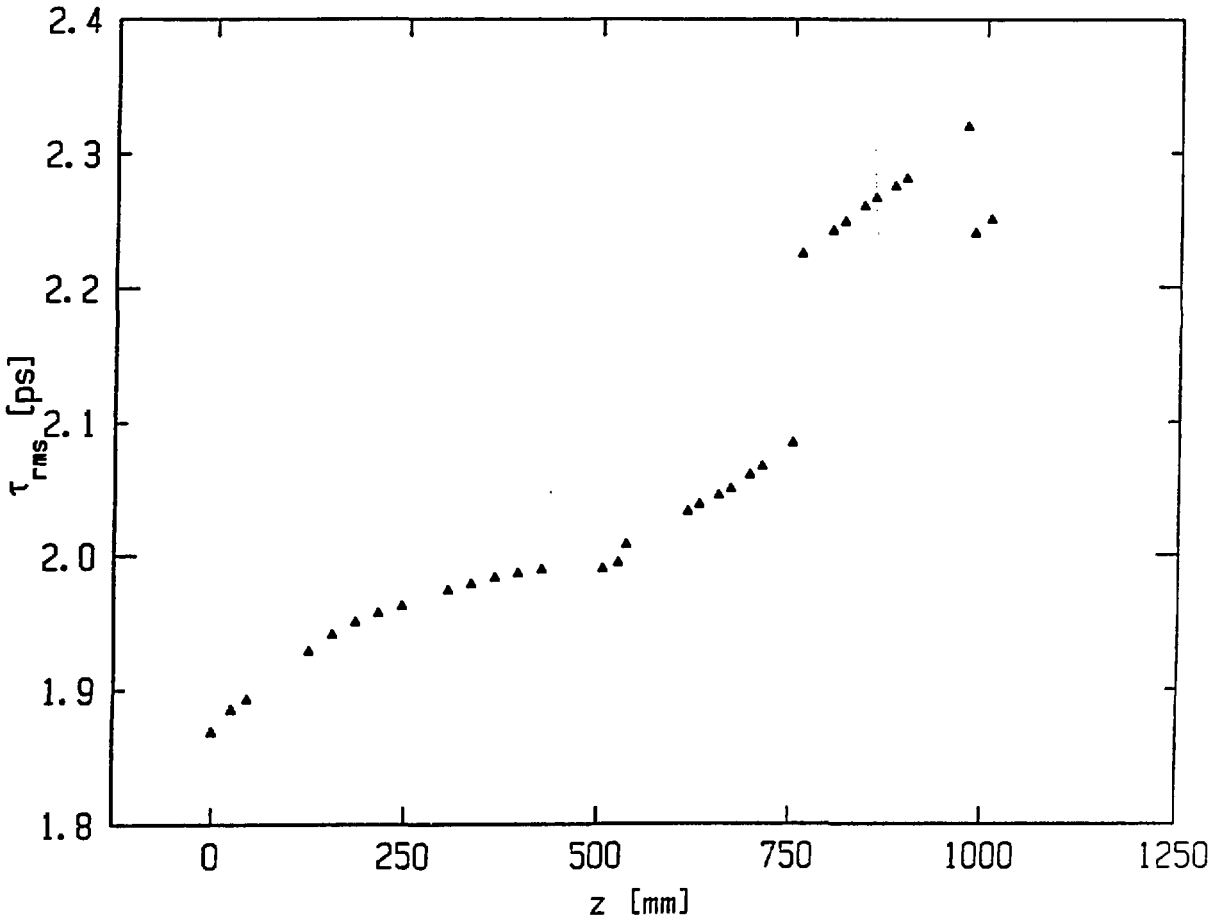

Figure 7: Pulse length in the injection line.

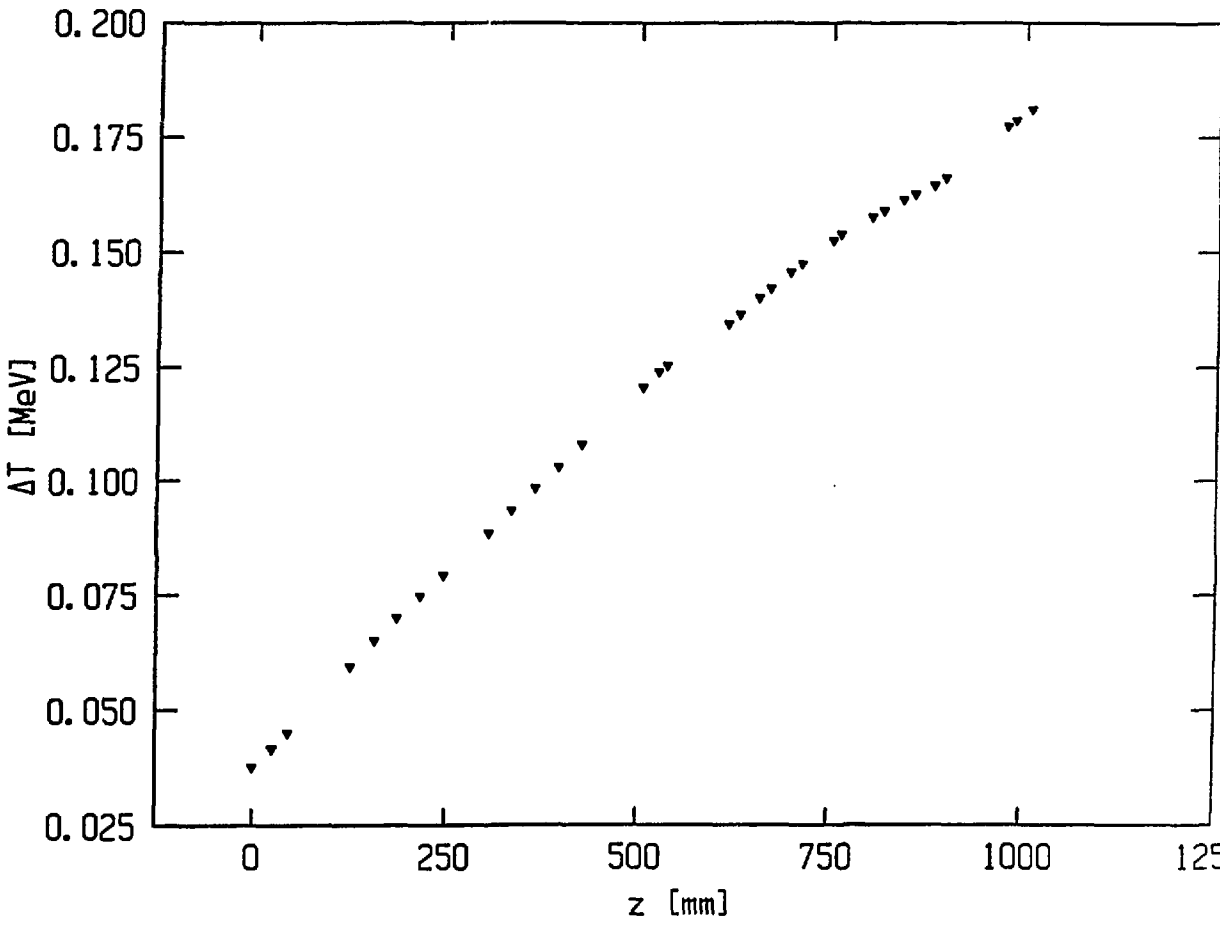

Figure 8: Energy difference in the injection line.

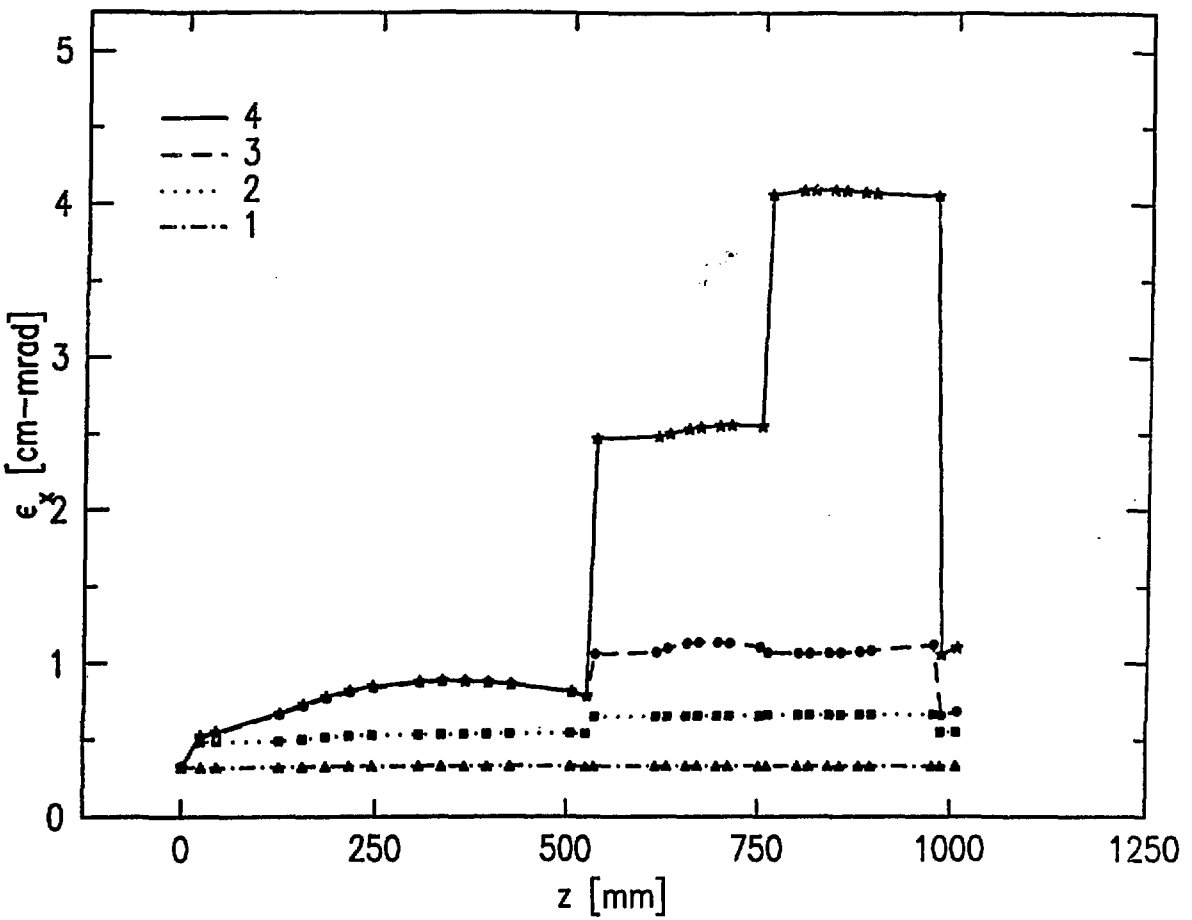

Figure 9: Horizontal emittances vs distance z.

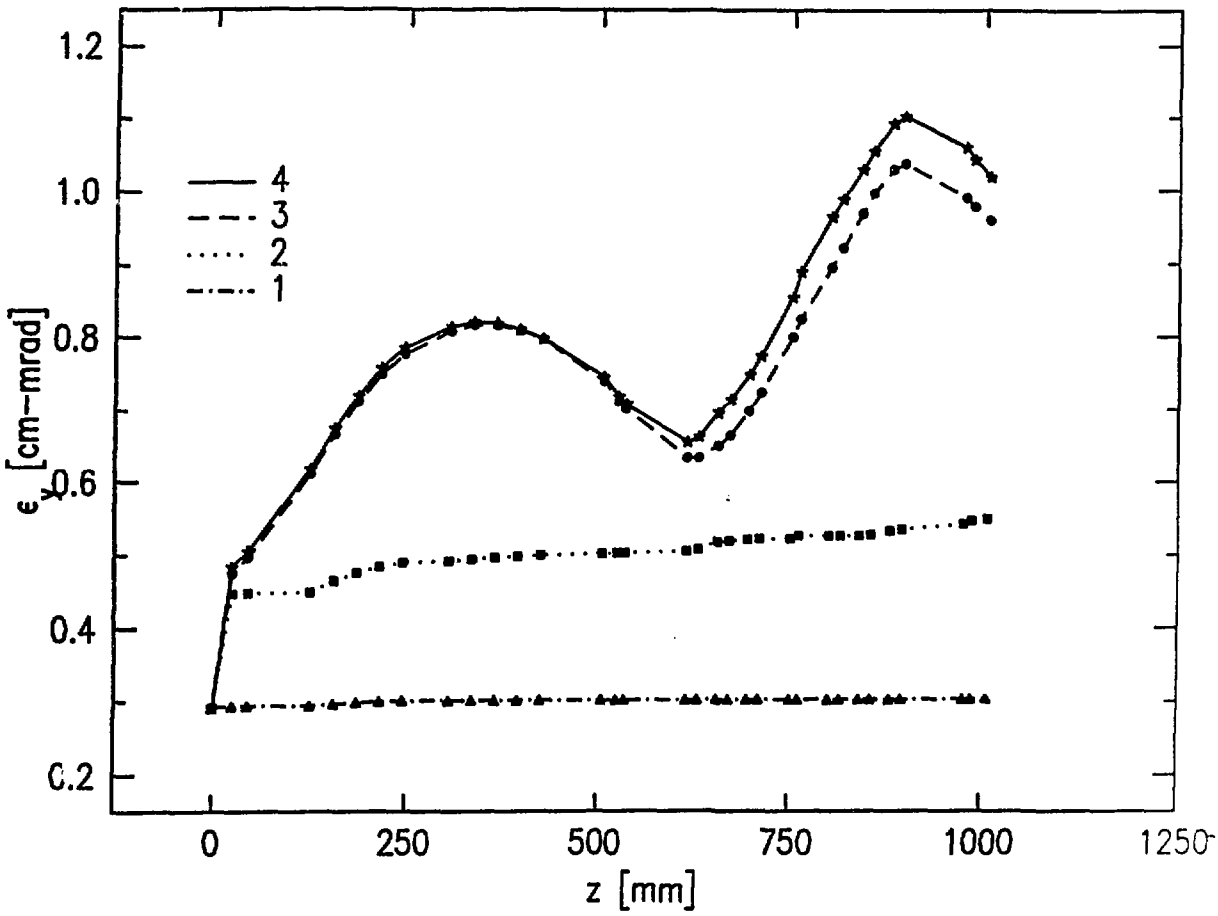

Figure 10: Vertical emittances vs distance z.

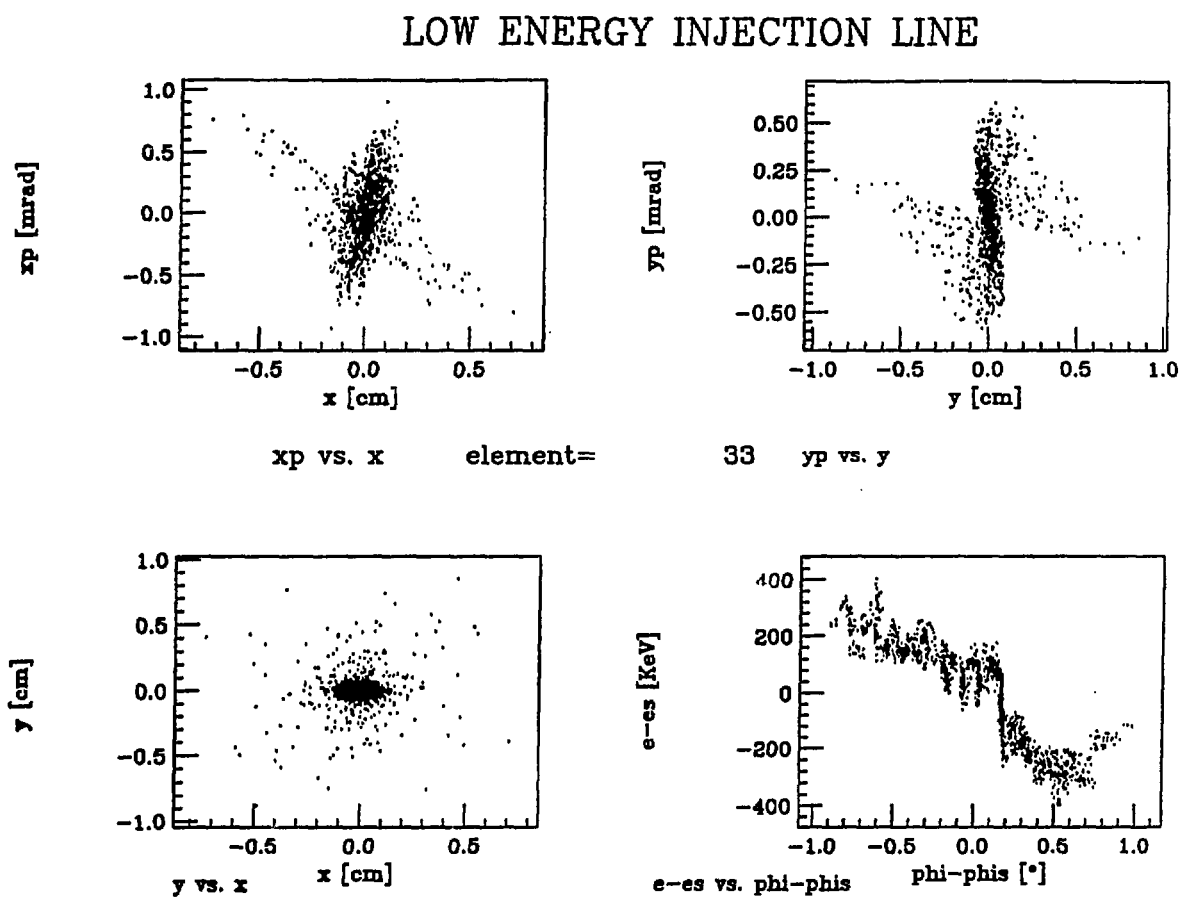

Figure 11: Phase space plots at the end of the injection line.